RESEARCH ARTICLE

A Unified Linear Self-Regulating Method for Active/Reactive Sustainable Energy Management System in Fuel-Cell Connected Utility Network

KAMRUL HASAN[1], **MUHAMMAD MURTADHA OTHMAN**[1], **(Member, IEEE),**
SHEIKH TANZIM MERAJ[2], **MASOUD AHMADIPOUR**[1],
M. S. HOSSAIN LIPU[3], **(Senior Member, IEEE), AND MOHSEN GITIZADEH**[4]

[1]School of Electrical Engineering, College of Engineering, Universiti Teknologi MARA (UiTM), Shah Alam, Selangor 40450, Malaysia
[2]Department of Electrical and Electronic Engineering, Universiti Teknologi PETRONAS, Seri Iskandar 32610, Malaysia
[3]Department of Electrical and Electronic Engineering, Green University of Bangladesh, Dhaka 1207, Bangladesh
[4]Department of Electronics and Electrical Engineering, Shiraz University of Technology, Shiraz 71557-13876, Iran

Corresponding author: Muhammad Murtadha Othman (mamat505my@yahoo.com)

ABSTRACT In fuel-cell-connected utility networks, electrical loads attached to the power network often generate reactive power, which hinders the utility from normal functioning and reduces the system power factor. This condition results in wasted energy, increase demand for electricity, system overload, and higher utility costs for customers. Besides, a power system's poor power factor is often caused by a large distorted reactive power element because of the widespread use of non-linear loads. Moreover, power outages were brought on by voltage dips resulting from reactive power. In a fuel cell-based network, traditional utilities often use classical filters that are unable to remove harmonic properties, and incapable of compensating for the reactive power. Moreover, power outage compensation is overlooked in most fuel cell-based energy systems. To address this problem, the proposed article provides a novel unified linear self-regulating (LSR) active/reactive sustainable energy management system (SEM) that can adjust the power factor by compensating for power outages and reactive power, and precisely removing harmonics from the electricity network. As a result, the suggested mechanism may avoid power losses and allow users to save money on their power costs. Furthermore, notwithstanding grid availability, the critical loads receive an uninterrupted power supply due to the automatic transition circuit implemented in the SEM. The suggested system's performance is evaluated under various load circumstances and the findings have shown that the suggested SEM can successfully decrease harmonics from the network while also keeping the power factor of the electricity network near unity.

INDEX TERMS Active/reactive power, fuel cell, microgrid, power quality, renewable energy, sustainable energy management system.

NOMENCLATURES
Abbreviations

AC	Alternating current.
DC	Direct current.

EFO	Electromagnetic field optimization.
FC	Fuel cell.
LPF	Low pass filter.
LSR	Linear self-regulating.
MFPA	Modified flower pollination algorithm.
MLI	Multilevel inverter.

HS	Harmonic search.
PEMFC	Proton exchange membrane fuel cell.
PFCPQ	Power factor correction active/reactive power.
PI	Proportional integral.
P-INV	Parallel inverter.
PLL	Phase-locked loop.
PQ	Active/reactive power.
PWM	Pulse-width modulation.
RES	Renewable energy source.
SEM	Sustainable energy management.
SOGI	Second-order generalized integrator.
THD	Total harmonic distortions.
W-H	Widrow-hoff.

Symbols

A	Amplitude.
C	Capacitance (μF).
C_{sync}	Power outage detection switch.
D	Duty cycle.
e	Exchange coefficient.
F	Faraday's constant (Cmol^{-1}).
f	Frequency (Hz).
G	Universal gas constant (JK^{-1} mol^{-1}).
H	Hysteresis band.
H_2	Hydrogen.
I	Current (A).
K	Gain.
l	Learning rate.
L	Inductance (mH).
L_i	Line inductance (mH).
N	Number of cells.
O_2	Air.
P	Active power (kW).
Q	Reactive power (kVAR).
R	Resistance (Ω).
r	Harmonic order.
T	Operating temperature (°C).
t	Time.
T_{sl}	Tafael slope.
V	Voltage (V).
W	Weight-function.
z	Number of electrons.

Subscripts

bc	Boost converter.
con	Constant.
$dc\text{-}link$	Direct current-link.
est	Estimated.
fc	Fuel cell.
fun	Fundamental.
g	Grid.
inj	Injected.
$L\text{-}L$	Line to line.
ocv	Open circuit voltage.
out	Output.
p	Phase.
pvl	Polarization voltage loss.

ref	Reference.
$sync$	Synchronization.

Greek

α	Error.
ω	Angular frequency.
θ	Phase-angle.

I. INTRODUCTION

In recent years, climate change concerns and the fast depletion of fossil fuels have made renewable energy sources (RESs) a hot topic. RESs are largely accepted to be environmentally friendly, cost-effective, and sustainable. Versatility, quiet operation, superior efficiency, and modular design of fuel-cell [1], [2], [3] have lately gained favor amongst RES technologies. Compared to wind and solar energy resources which are intermittent in nature, fuel cells improve the overall system effectiveness in relation to power control and stability [2]. Recently, utility-interfaced fuel cell solutions have been included for three-phase and single-phase electrical networks [4], [5]. A grid-connected fuel cell system refers to the unification of fuel cells with the electricity network. This architecture of the network is used to reduce the consumption of electric power from the electrical networks. Nearby loads (such as lighting and heating) may consume the power generated by the fuel cell system, or the electricity can be traded to the electricity-distributing corporations. Moreover, the fuel cell can support sensitive loads during power outages [6], [7], [8].

Nowadays, most of the power industries are also shifting their emphasis from conventional energy toward sustainable energy like fuel cells, considering the facts of global environmental pollution [9]. Therefore, the implementation of fuel-cell-based power generation has increased tremendously in the industry sector, decreasing the high dependency on fossil fuel resources [10], [11], [12]. In order to strengthen the electric grid and reduce abrupt fluctuations in the utility grid, fuel cell energy systems are placed strategically close to a distribution line [13]. This increases the safety and efficiency of the utility grid. In this context, the regulated interface devices provide the electric grids with the electrical energy generated by the fuel cell stacks. A collective power exchange between the local load and the grid supply is ensured by the grid-connected fuel cell system. These systems must successfully maintain the power quality of a grid that may include optimal energy flow, minimal harmonic distortion, and safe operation to customers. However, a number of local loads, including transformers, electrical devices, inductors, and capacitors, whose currents exhibit phase inequality with respect to voltage, degrade the electrical systems' power quality [14]. The smooth operation of the power industry requires finer power quality. In recent years, various fuel-cell-based sustainable energy management systems (SEM) have been developed and proposed by researchers to enhance

the power quality of the grid. There are several international standards regarding the power quality requirement. Among them, the US energy division affiliated with Energy Star recommends that the power factor for the distribution network must be more than 0.9 p.u. (per unit) [15]. Additionally, the IEEE 519 standard states that the total harmonic distortion (THD) should be less than 5% [16]. Moreover, the effect of reactive power on local inductive loads is more apparent and is known to put transmission parts in the electrical grid in danger of overloading and overheating. This problem can be solved by correcting the reactive power by reducing the harmonic contents and keeping up the current and voltage by compensating for power outages and reactive power for the utility grid with a unity power factor. A suitable SEM is thus needed to address these problems.

Recent research has looked at a number of SEMs to improve the power quality of fuel cell-attached grid configurations for various purposes. In order to lessen the harmonic in the utility, The THD profile of the grid is considered by Azzeddine et al. [17] using a conventional PQ technique to suppress the current harmonic and compensate for reactive power. A. Mojallal and Lotfifard [18] examined load management as a means of achieving excellent steady-state energy efficiency. This study used a predictive control economic model without considering phase inequality or harmonics. Likewise, Zhu et al. [19] introduced a control method based on the virtual synchronous generator to deal with transients and high power demand. However, the harmonic profile of the grid current, power outage, and power factor correction was not considered in the paper. Especially, in the presence of nonlinear load, the grid current is affected noticeably which increases the overall total harmonic distortion (THD). Nonetheless, the control algorithm lacks performance significantly during phase inequalities and power outages since the incorporated conventional phase-locked loop (PLL) is unable to perform well during phase distortion and grid voltage variations [20], [21]. LCL filters were utilized to separate the harmonic content which is bulky and incompetent to different types of nonlinear loads. Besides, power factor correction was also overlooked. Apart from the conventional inverter, a multilevel DC-AC converter is also utilized in the fuel cell integrated grid system by Priya and Ponnambalam [22]. Although multilevel inverter (MLI) must perform better than the conventional inverter technology, the THD profile is not satisfactory for linear loads. Non-linear loads were not considered, and grid distortion and power outages were also not considered in this study.

Table 1 illustrates the active/reactive power features of a few recently suggested controls for fuel-cell-connected utility networks. Aguirre et al. [23] make a comprehensive hydrogen-based grid system proposal that combines fuel cells and water electrolysis. Only optimal circumstances have been used to assess the system's dynamic responsiveness. The power factor adjustment was not given any thought or study despite the system's intricate nature. The implementation

of a vector proportion integral (PI) controller to carry out harmonic correction is found in [24]. Although the system was not tested under challenging circumstances like voltage fluctuations or disruptions, the result demonstrated a good decrease in harmonic elements Additionally, it used a traditional PLL, which has a number of performance problems such as phase disruptions, phase shifts, higher computational demands, and complicated configuration [20], [21]. To utilize the PI control operation in the SEMs, a fine-tuning approach plays an important role and to fine-tune the PI controller settings and increase its effectiveness, a control system is presented by Mosaad and Ramadan [25]. It utilized three optimization techniques: electromagnetic field optimization (EFO), modified flower pollination algorithm (MFPA), and harmony search (HS). There are several research on fuel cell energy management based on reinforcement learning (RL) [26]. However, most researched RL algorithms suffer from overestimation flaws and to solve this, an energy management scheme based on the Double Q-learning algorithm [27] was proposed with state constraint and variable action space as a means to address these issues and attain an online power distribution system with the nearly optimum operational economy. In order to operate a power station powered by fuel cells optimally, coordinated control techniques have been utilized by Sun et al. [28]. Although the system's total THD was effectively reduced, it did not take into account non-linear loads or harmonically contaminated grid voltage situations. Investigating the dynamic performance of voltage sag/swell situations was done using the improved PI control. The system's transient response was improved, but it still has some serious flaws, including computational complexity brought on by the use of three distinct optimization strategies, failure to meet the minimal harmonics specification due to the use of a traditional low pass filter (LPF), and a lack of investigation on power factor improvement.

Moreover, Qi Li et al. [37] proposed a model predictive control-based energy management scheme integrating self-trending prediction and the subset-searching algorithm to implement the real fuel cell hybrid system, enhance the efficacy of fuel cells, and lower the operational expenditure. A PLL-free structure was employed by Sabir [34] in a grid-attached fuel-cell unit to address power quality issues. Even though this strategy effectively avoided PLL's disadvantages, it used repeating LPFs to address power quality difficulties in unbalanced grid situations. Furthermore, as it primarily emphasizes power factor adjustments of the fuel-cell attached utility network, harmonic mitigations were not investigated. The same strategy was used by Inci [35], where a unique control known as the PFCPQ strategy was devised to address solely the phase disparities on the utility network. To compensate for reactive power, this arrangement utilized PLL. The use of a similar strategy is shown in [36]. The fact that other FC systems were not evaluated under power outage conditions, except for the FC system produced in [25], [38], [39], and [40] which considered voltage imbalance condi-

TABLE 1. SEM features in different fuel-cell-connected utility networks.

Scope	Significances	Knowledge gap	Filters	References
1. Harmonic mitigation. 2. Quicker transitory reaction.	1. Effective optimization of PI specification. 2. A quicker transient reaction was attained. 3. THD complies with IEEE 519 in optimal situations.	1. Complicated mathematical expressions 2. Complicated architecture 3. THD failed to fulfill the IEEE 519 specification when evaluated during un-ideal situations. 4. LPFs are included. 5. The capability of power factor adjustment was not verified.	LPF	[29], [23]
1. Tackling transient event 2. Supporting high power demand	1. A small signal model of the parameter design was introduced. 2. Negative sequence voltage was suppressed and separated.	1. The THD profile of the grid was not discussed. 2. Power outages and voltage variations were not studied.	SOGI	[19]
1. Harmonic mitigation 2. Reactive power compensation	1. THD quantity was reduced moderately. 2. The reactive power was compensated moderately.	1. The power factor profile was not studied. 2. Incorporated conventional PLL. 3. Utilization of LCL-type passive filter.	LCL	[17]
1. Harmonic mitigation	1. THD quantity was reduced moderately for both voltage and current.	1. Nonlinear loads were not considered. 2. Grid voltage variations were not studied.	LCL	[22]
1. Harmonic mitigation	1. Superior to the traditional PI-based PQ method in terms of harmonic mitigation. 2. Utilizing the resonant current control loop results in a quicker transitory reaction.	1. During extreme grid voltage levels, the system has not been validated. 2. The capability of power factor adjustment was not verified. 3. Complicated architecture 4. PLL was included.	Vector-PI	[24]
1. Improving the performance of fuel cells. 2. Harmonic reduction.	1. The fuel cell's performance was brought up to its optimal level. 2. In circumstances of ideal load, a successful minimization of the system's total THD was achieved.	1. There was no consideration given to the harmonically contaminated grid voltage state. 2. There was no consideration given to non-linear loads. 3. The ability to compensate for the power factor was not confirmed.	Optimized-PI	[25], [28], [30]
1. Performance improvement for fuel cells. 2. cost reduction	1. The fuel cell operates at its peak efficiency. 2. The system's total cost was kept to a minimum.	1. The capacity to eliminate harmonics was not verified. 2. The ability to compensate for the power factor was not verified. 3. Consists of LPFs.	LPF	[31]–[33]
1. Resolving issues with power quality	1. PLL less control design. 2. No reactive power was delivered from the utility. 3. Improvement of the power factor.	1. The capacity to eliminate harmonics was not verified. 2. Consists of LPFs. 3. Considering non-ideal loads, the capacity to compensate for the power factor was not proven.	Repetitive LPF	[34]
1. Resolving issues with power quality	1. Grid reactive power flow was prevented. 2. The power factor was adjusted appropriately for both ideal and non-ideal loads.	1. The capacity to eliminate harmonics was not verified. 2. PLL was included in the structure.	PI	[35], [36]

tions, is a significant finding from the literature study that needs to be addressed. Since voltage imbalance power quality issues especially power outage issues can greatly affect the overall power quality, the power factor, and efficiency of the fuel-cell connected power network, ignoring it creates great instability in the system.

The literature research makes it clear that the majority of the abovementioned research works are not fulfilling several major power quality requirements in the fuel-cell connected utility network by ignoring the power outages, and voltage sag/swell power quality problems that greatly affect the overall power quality and power factor. The unified linear self-regulating (LSR) control method along with the power outage

detection circuit is thus suggested in this manuscript. It is able to maintain nearly unity power factor as well as limit the THD of supply current by 5% during challenging situations faced by load or grid conditions and compensate for power outages, enabling the technology to be used and implemented in industrial settings. Moreover, the unified nature of the LSR control is another important feature of the proposed method.

This manuscript provides a viable solution for multiple power quality issues regarding critical loads. The proposed SEM consists of a power outage detection circuit that can detect power outage situations and can support critical loads using fuel-cell power. Each operation (three operations in total) is attained by the identical type of LSR algorithm.

Furthermore, faster frequency estimation is essential in fuel-cell-connected grid applications where the frequency is prone to change in a relatively large range. Another important feature of the proposed unified LSR technique is that all three LSR units operate using the same input vector and thereby diminish the computational burden of the overall system configuration.

The merits of the proposed method can be summarized as follows:

I) A unique sustainable energy management system (SEM) along with a power outage detection circuit is developed considering the future trends of energy management systems for fuel-cell connected utility networks.

II) In order to reduce the computational burden of the overall control system, each task of the SEM control algorithm is implemented with one identical LSR control module.

III) Several LSR controllers are utilized in a unified manner for conducting multiple operations such as harmonic reduction, power factor improvement, limiting the unnecessary outflow of reactive power from the utility, and power outage compensation without using conventional PLLs and LPFs.

IV) Furthermore, in terms of performance evaluation of the unified LSR-based SEM, the dynamic response in all the case studies is intensely scrutinized.

The manuscript is arranged into five sections. Section II describes the modeling of the fuel-cell-connected utility network. The SEM based on unified LSR algorithms is reported in section III. The performance investigations and discussion, and comparative assessments are covered in section IV. Finally, section V offers the findings of the proposed study.

II. FUEL CELL CONNECTED GRID SYSTEM CONFIGURATION

Power from fuel cells is converted from direct current (DC) to alternating current (AC) before being sent to the power grid. The power-producing sources are combined with sub-components in order to transform the energy. These parts are in charge of the fuel-cell-connected utility network's practical management and DC-to-AC conversion. The DC-AC operating device is referred to as an inverter [41], [42], [43]. The grid receives its active power from fuel cells through the parallel-connected inverter. Additionally, the parallel inverter (P-INV) is responsible for controlling the flow of reactive power between the grid and fuel cells. Furthermore, the power outage is also compensated by the P-INV. However, the DC-DC converter is employed inside the fuel-cell-connected utility network to keep the fixed desired voltage output below 5% of its standard voltage rates. As a result, the converter and the inverters are essential components of the fuel-cell-connected utility network. The circuit configuration of the fuel-cell-connected utility network is shown in Fig. 1, which also shows the overall structure of the proposed system. A boost (DC-DC) converter, fuel-cell power source, P-INV, a control switch to detect power outage, and a passive filter to improve the quality of the power at the grid's edge, and domestic loads

TABLE 2. Principle parameters for grid and load.

Parameters	Symbol	Value
Line to Line voltage	$V_{L\text{-}L}$	400 V
Grid frequency	f	50 Hz
Line inductance	L_i	1 mH
Non-linear load	$R - L$	50 Ω – 50 mH
Load 1	$R_{l1} - L_{l1}$	55 Ω – 36 mH
Load 2	$R_{l2} - L_{l2}$	35 Ω – 55 mH
Load 3	$R_{l3} - L_{l3}$	45 Ω – 40 mH

make up the structure's subcomponents. The overall system is called the P-INV-FC system in this manuscript.

A. MODELING OF UTILITY NETWORK AND LOAD

In the stated system, the fuel-cell power source unit is connected to a three-phase utility network with specifications of 400 V_{L-L} /50 Hz. Two different kinds of loads are linked to the utility network depending on the sort of proposed system's operational investigation. In the first investigation, a resistive-inductive load (R- L) supplied by an unregulated bridge rectifier linked to the utility network serves as a three-phase nonlinear load that consumes active and reactive power. To evaluate the harmonic removal capabilities of the proposed system, this load bank is attached. Fig. 2(a) depicts the internal organization of the non-linear load. In the second investigation, three distinct R-L loads are attached to the utility network to evaluate the network's capacity to rectify the power factor. Each of the loads is linked to a separate circuit breaker, which enables them to operate at various times. Fig. 2(b) provides an illustration of this load bank's interior construction. Table 2 displays the values of these parameters for further explanation.

The linked loads have a major impact on the electrical output values of systems using fuel cells that are connected to the grid. Two problems are particularly significant among the many ways that loads may impair the operation of fuel cells. The first problem is brought on by changes in loads, either gradual or abrupt, whereas the second problem is produced by ripple current that is often brought on by loads of non-linear type.

The system's coupled non-linear loads generate extra ripple currents. The fuel cells are especially vulnerable to damage from low-frequency ripple currents. Utilizing the fuel-cell connected utility network to provide lower-frequency AC electricity to the load, the fuel-cell arrangement produces lower-order harmonic elements in the grid current. In the presence of a harmonically contaminated current, the flow of the fuel must be regulated to a maximum rate, which leads to fuel waste, higher energy expenditures, poor performance, and low efficiency. As a result, the fuel-cell-connected utility network needs an SEM that can reduce the existence of the low-order harmonic or ripple current.
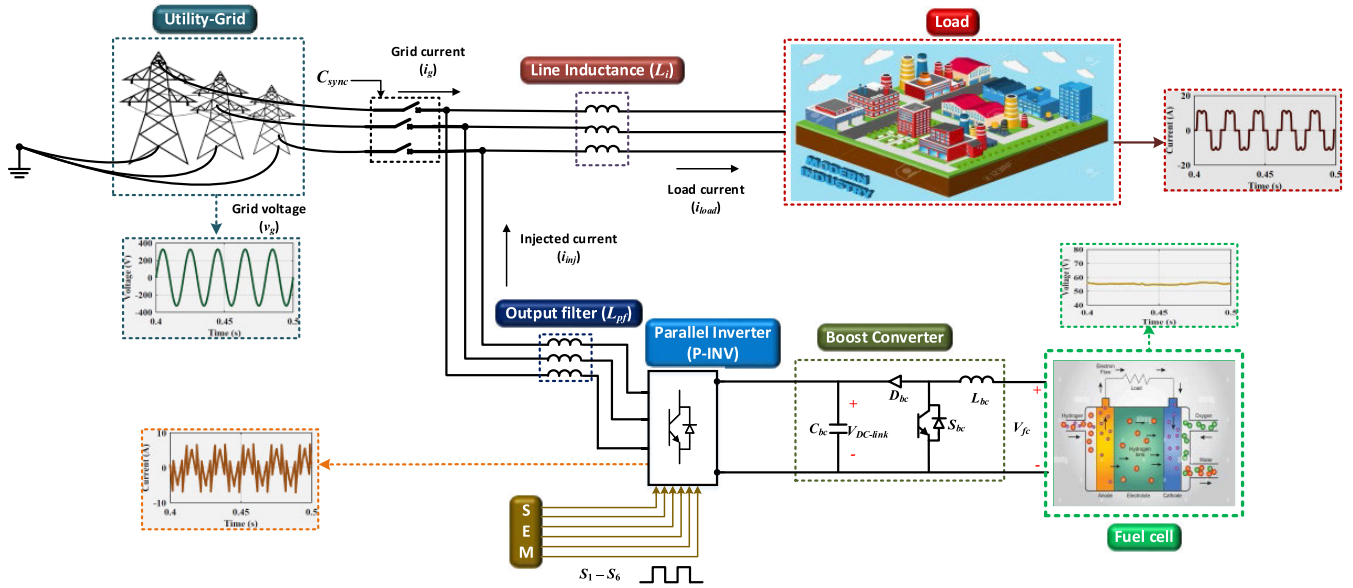
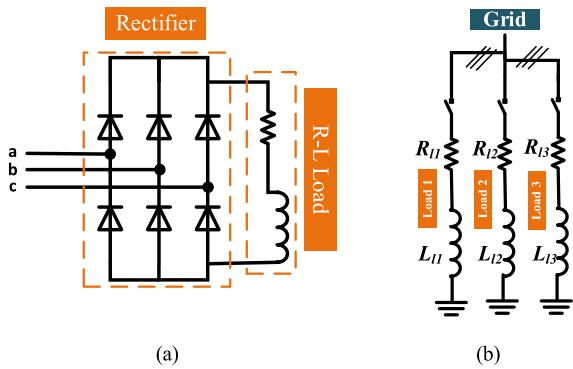**FIGURE 1.** The electrical design of fuel-cell connected utility network.

FIGURE 2. Load banks to assess the capacity to (a) reduce harmonics and (b) rectify power factor.

FIGURE 3. Diagram of a PEMFC equivalent circuit.

B. MODELING OF FUEL CELL

A proton exchange membrane fuel cell (PEMFC) is used for the proposed investigation. When it comes to power production, PEMFC is the most widely used form of a fuel cell. PEMFC has the ability to provide a large output current at low voltages (<50 V). The analogous circuit of the PEMFC is shown in Fig. 3. The PEMFC's operating concept is shown in (1) to (6) [23]. The fuel cell's equivalent output potential is described as:

$$V_{fc} = V_{ocv} - V_\Omega - V_{pvl} \tag{1}$$

Here, V_{fc} denotes the fuel cell stack voltage output, V_{ocv} denotes the open circuit voltage, V_Ω denotes the ohmic voltage loss, V_{pvl} denotes the polarization voltage loss.
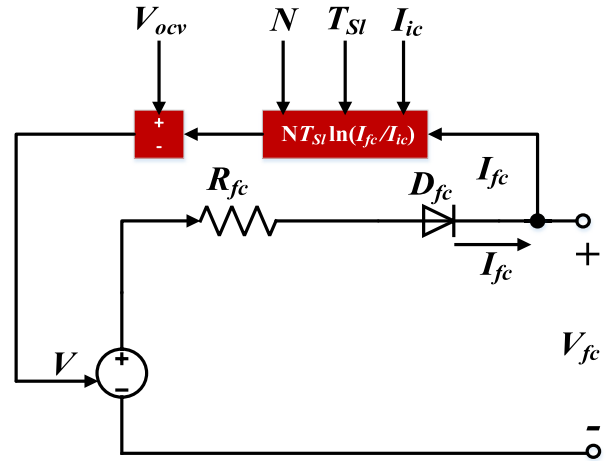
The fuel cell's open-circuit potential value is regarded as [35]:

$$V_{ocv} = V_{con}\left[1.229 + (T - 298)\frac{-44.43}{zF} + \frac{GT}{zF}ln\left(P_{H_2}P_{O_2}^{\frac{1}{2}}\right)\right] \tag{2}$$

Here, V_{con} denotes rated voltage constant, T denotes operating temperature, F denotes Faraday constant, G denotes gas constant, P_{H2} and P_{O2} denote the gas pressure, z denotes transfer electron number. In standard pressure, the electromotive force is selected as 1.229.

The ohmic voltage loss can be expressed as [35]:

$$V_\Omega = I_{fc} \times R_{fc} \tag{3}$$

TABLE 3. Fuel cell specifications.

Specifications	Symbol	Value
Nominal voltage	V_{fc}	45 V
Nominal Current	I_{fc}	133.35 A
Nominal power	P_{fc}	6 kW
Maximum voltage	V_{max}	37
Maximum current	I_{max}	225
Maximum power	P_{max}	8.32kW
Cells number	N	65
Operational temperature	T	338 kelvins
Central resistance	R_{fc}	0.07833 Ω
Universal gas constant	G	8.315 JK^{-1}mol^{-1}
Interchange current	I_{ic}	0.29197 A
Interchange coefficient	e	0.60645
Number of electrons	z	2
Faraday's constant	F	96485 Cmol^{-1}
Standard voltage	V_{st}	65 V
Pressure of fuel supply	P_{H2}	1.5 bar
Pressure of air supply	P_{O2}	1 bar

TABLE 4. Inverter and DC-DC converter specifications.

Specifications	Symbol	Value
Duty cycle	D	0.45
Proportional gain	$K_{p\ bc}$	0.005
Integral gain	$K_{i\ bc}$	0.15
Inductor	L_{bc}	0.5 mH
Capacitance	C_{bc}	3300 uF
Reference voltage	$V_{bc\ ref}$	330 V
Passive filter	L_{pf}	5 mH

where, R_{fc} is the inner resistance of a stack, i_{fc} is the fuel cell output current.

The total polarization overvoltage V_{pvl} can be represented as:

$$V_{pvl} = N \times T_{sl} \times ln\left(\frac{i_{fc}}{i_{ic}}\right) \tag{4}$$

where N is the number of cells. The Tafel slope T_{sl} and the exchange current i_{ic} in (4) can be expressed as follows [35]:

$$T_{sl} = \frac{GT}{zeF} \tag{5}$$

$$I_{ic} = \frac{zFk\left(P_{H_2} + P_{O_2}\right)}{Gh} e^{\frac{-\Delta G}{GT}} \tag{6}$$

where, k is Boltzmann's constant, and h is Plank's constant.

The NedStack PS63 from NedStack's datasheet is used to create a model of a 6kW-45V PEMFC stack which can be found in [44]. According to the datasheet, the variables used are shown in Table 3.

As illustrated in Fig. 4, the polarization curves of the selected model are derived in a steady state based on the datasheet. It is noted that the simulated characteristic curves perfectly replicate the genuine one shown in [44], which signifies the fuel cell modeling accuracy. For the FC system, Fig. 4 represents that the PEMFC's nominal power rating is 6 kW at rates of 133.3 A and 45 V. The maximum output is 8325 W at the highest operational parameters of 225 A/37 V.

C. MODELING OF INVERTER AND CONVERTER MODULE

Given the fuel cell's dynamic properties, a DC-DC converter is necessary for increasing and stabilizing the voltage output while maintaining optimal effectiveness. Delivering consistent voltage to the common DC-link of the inverters is the main goal of the DC-DC converter [45]. The DC-link voltage in this research is managed through PI control. The designated reference voltage and the actual voltage quantity are both monitored by the PI control. Using the pulse width modulation (PWM) technique, the PI control's output creates

a pulse that activates the switch [46]. The DC-link voltage is expressed as ($V_{DC-link}$) according to the duty cycle (D) or switching period.

To integrate with the grid, the converter output, which has a steady DC voltage, is transformed into an AC output voltage. A parallelly connected inverter is used on the grid to transform DC electricity into AC power. Since inverters are a crucial component of the interface, they are positioned after the DC-DC converters. This system uses a typical three-level inverter using parallel construction, and the main purpose of the parallel inverter is to mitigate the source current harmonic, maintain the unity power factor, to compensate for the power outage. Odd harmonic components of the output voltage value (V_{out}) are examined via Fourier analysis. Following is an example of an expression for the inverter's output voltage:

$$V_{out}(\omega t) = \sum_{r=1}^{\infty} A_r \sin(r\omega t) \tag{7}$$

$$A_r = \frac{4V_{DC-link}}{r\pi} \sum_{r=\text{odd}} \sin(r\omega t) \tag{8}$$

It is important to highlight that all the literature on parallelly connected inverter fuel-cell connected grid systems showed harmonic reduction and power factor correction. However, none of them emphasize power outage conditions or deep voltage sag conditions. Based on the inverter, the appropriate control strategy is implemented. As a result, the inverter's main objective is to manage the energy flow in the fuel-cell-connected utility network. A straightforward passive filter is utilized [47] to remove ripples from the voltage source inverter's switching operation. The specifications of the inverter and the dc-dc converter in the suggested arrangement are fully detailed in Table 4.

III. UNIFIED LINEAR SELF REGULATING (LSR)-BASED SUSTAINABLE ENERGY MANAGEMENT SYSTEM (SEM)

The functions of unified LSR can be classified into four main categories which are:
- Reference load current generation for Parallel Inverter (P-INV)
- Phase synchronization of reference current for P-INV
- Reference load voltage production for P-INV throughout the power outage operation

An improved Widrow-Hoff (W-H) algorithm is utilized to update the weights of the LSR algorithms. Two weight values are considered in the mechanism of the LSR. Since the
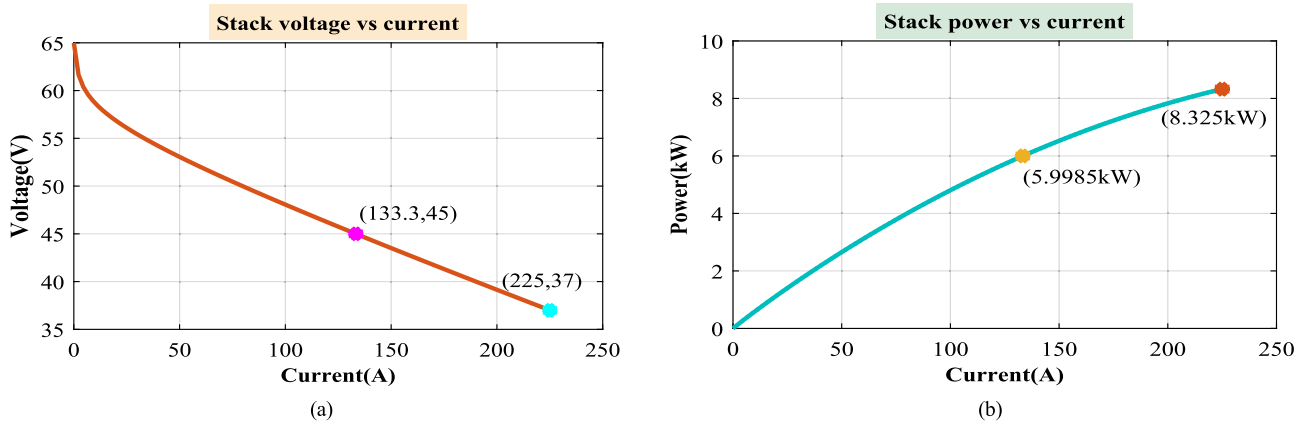
FIGURE 4. The fuel cell unit's characteristic curves: (a) stack voltage vs current, (b) stack power vs current.

number of weight values is limited to two, the estimation process reflects accuracy, fast response, and high adaptability. The algorithm for the LSR weight update mechanism can be expressed as follows:

$$\bar{W}\,(updated) = \bar{W}\,(old) + \frac{l\alpha Z}{Z^T Z'} \qquad (9)$$

$$\bar{W}(old) = \begin{bmatrix} W_{1s} \\ W_{1c} \end{bmatrix} \qquad (10)$$

$$Z = \begin{bmatrix} \sin(\omega t) \\ \cos(\omega t) \end{bmatrix} \qquad (11)$$

where Z indicates the fundamental sine and cosine functions. The error is indicated by α which is computed in each operational loop by subtracting the measured signal (s_{me}) from the estimated signal (s_{es}). The weights W_{1s} and W_{1c} indicate the sine and cosine function weights, respectively. The weights are updated depending on the error and implemented on the following operational loop $\bar{W}\,(updated)$. In this way, the latest value of the estimated signal (s_{es}) is achieved, and the resultant error is decreased. A learning rate (l) in a range of $0 < l < 1$ is utilized to achieve a stable error estimation with a stable convergence rate. The trial and error technique has been used to find the optimal value of learning rate (l) for the P-INV configuration and the value is considered to be 0.0001 [48]. Thereby, the estimated signal can be stated as follows:

$$s_{es} = W_{1s} \sin(\omega t) + W_{1c} \cos(\omega t) \qquad (12)$$

where estimated signal magnitude (M_{es}) can be calculated as:

$$M_{es} = \sqrt{W_{1s}^2 + W_{1c}^2} \qquad (13)$$

A. LSR-BASED SYNCHRONIZER
One LSR is utilized for the synchronization. For that purpose, the magnitude ($V_{gfun(es)}$) is extracted from the fundamental voltage ($v_{gfun(es)}$) in (15) and then divided by the grid voltage (v_g) to acquire the sine function ($sin(\omega t + \theta_p)$) in (16) which will perform the synchronization operation in between the reference current and grid voltage. In other words, it can be

considered a synchronizer that has a similar function as PLL. The sine function can be formulated as follows:

$$v_{gfun(es),p} = W_{1s} \sin(\omega t) + W_{1c} \cos(\omega t) \qquad (14)$$

$$V_{gfun(es),p} = \sqrt{W_{1s}^2 + W_{1c}^2} \qquad (15)$$

$$\sin(\omega t + \theta_p) = \frac{v_{g,p}}{V_{gfun(es),p}} \qquad (16)$$

Here, θ_p represents the phase angle of phases *a, b, or c*. By examining and contrasting their dynamic responses, it is possible to see how the LSR is better than traditional PLL. The main distinction between LSR and PLL is how they operate. In contrast to standard PLL, which removes harmonic components from harmonically contaminated signals, the suggested LSR extracts fundamental components. Meanwhile, in LSR, the fundamental grid voltage magnitude is extracted and then divided by the grid voltage signal to acquire the phase information which will perform the synchronization operation. LSR performs an update of weight functions after removing the fundamental component in order to produce the required signal. Instead, PLL subtracts the required signal from the harmonically contaminated input.

Fig. 5 displays the frequency responses of the LSR and traditional PLL for harmonically contaminated signals. The frequency response of the traditional PLL may be seen to have reached its steady position after 0.34 seconds. Moreover, two different disturbances are introduced at 0.5 seconds and 0.7 seconds for a better understanding of the performance. A closer look reveals that PLL still has a frequency fluctuation at 0.5 seconds and an overshoot of 70 Hz at 0.7 seconds. Due to LPF's inadequate filtering capabilities, this happens. Increasing the order of the filter or using more sophisticated filters, for example, the Moving Average, Weiner, Chebyshev, Kalman, and others, may fix the problem. To handle increasingly challenging grid circumstances, these filters often need to be modified further since this procedure might create mathematical complexity. Additionally, very complex trigonometric computations are needed for these procedures. On the other hand, the frequency response of LSR is consistently
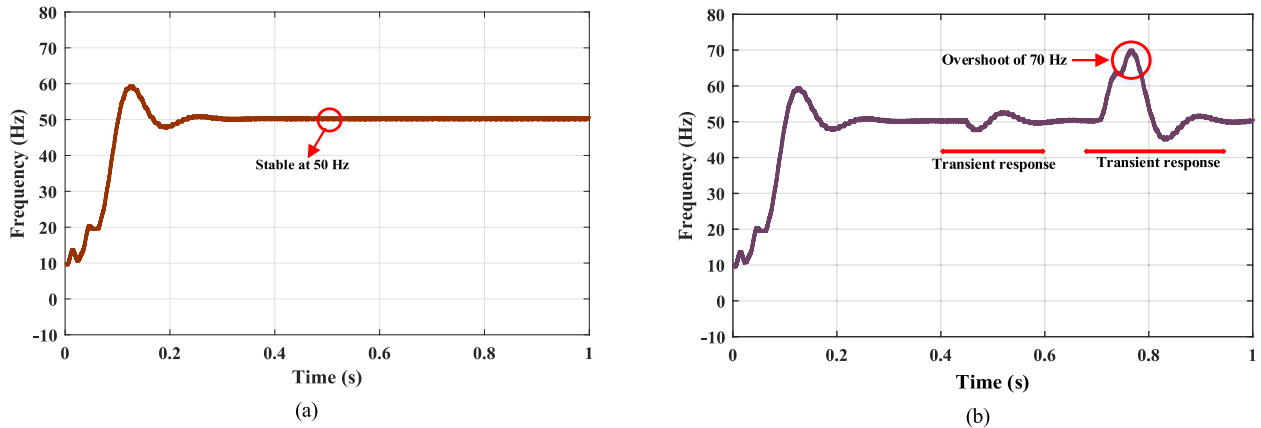
FIGURE 5. Frequency response of (a) LSR and (b) PLL during the distorted signal condition.

constant after it becomes stable at 0.3 seconds when there is harmonic signal pollution. During the 2nd and 3rd disturbances, LSR shows consistent performance and becomes constant at 50 Hz, unlike the traditional PLL fluctuations that occurred during the 2nd and 3rd disturbances. Since the LSR simply extracts the fundamental component, it doesn't need to be modified in any way depending on how severe the grid conditions are. Due to this, LSR has an additional functional benefit over traditional PLLs.

B. LSR-BASED ALGORITHM FOR P-INV

1) CONTROL CIRCUIT FOR POWER OUTAGE DETECTION

The two-mode performance of the proposed configuration which is the normal operating mode and power outage mode is decided by the control circuit for power outage detection. Several parameter settings are utilized for the main operation of this control circuit and the decision can be made whether the system is running in normal operating or power outage mode. The control circuit is integrated with P-INV to ensure a smooth transition between the two operating modes of the proposed unified LSR-based P-INV-FC configuration. Three conditional parameters (frequency, amplitude, and modes of operation) are utilized to generate the final decision (C_{sync}) of the control circuit. Note that the phase comparison between the two modes is not taken into consideration since the LSR algorithm will make sure the injected phase always follows the desired grid voltage phase. The schematic block diagram of the proposed control circuit is shown in Fig. 6.

The parameters setting is determined as follows:

- The variation in frequency in the middle of supply and reference voltage.
- The variation in magnitude in the middle of supply and reference voltage.
- A feedback command depends on the operational mood.

It can be noticed from Fig. 6 that in the course of power outage mode, if the grid appears, the control circuit confirms that the variation in frequency in the middle of the reference voltage and supply voltage is lesser than 0.3Hz and the variation
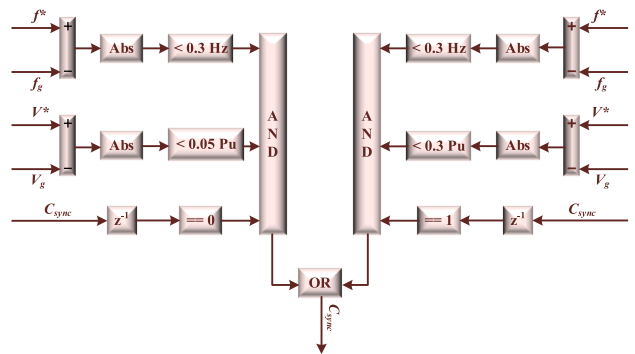

FIGURE 6. Schematic block diagram of the control circuit of power outage detection.

in magnitude is lesser than 0.05pu. An AND block receives these conditional analyses. However, for the reversed context that is the grid disappearance situation, the control circuit investigates the conditions where the magnitude variation is 0.3pu instead of 0.05pu which is used in the previous condition. Another AND block receives the conditional analysis. In the end, an OR block receives outputs from both AND blocks and the ultimate decision is made by the control circuit. The control circuit generates $C_{sync} = 1$ in the normal operating mode and $C_{sync} = 0$ in the power outage mode.

2) LSR-BASED HARMONIC REDUCTION

Fig. 7 depicts the P-INV control operation. The P-INV can be designated as the current modulator in the normal operational mode. LSR algorithm generates the estimated load current ($i_{load\_fun(es)}$). Here, one identical LSR module is utilized for each phase in the distorted load current (i_{load}) to extract the fundamental component. Thereby, (12) and (13) can be written as:

$$i_{load\_fun(es),p} = W_{1s} \sin(\omega t) + W_{1c} \cos(\omega t) \qquad (17)$$

$$I_{load\_fun(es),p} = \sqrt{W_{1s}^2 + W_{1c}^2} \qquad (18)$$

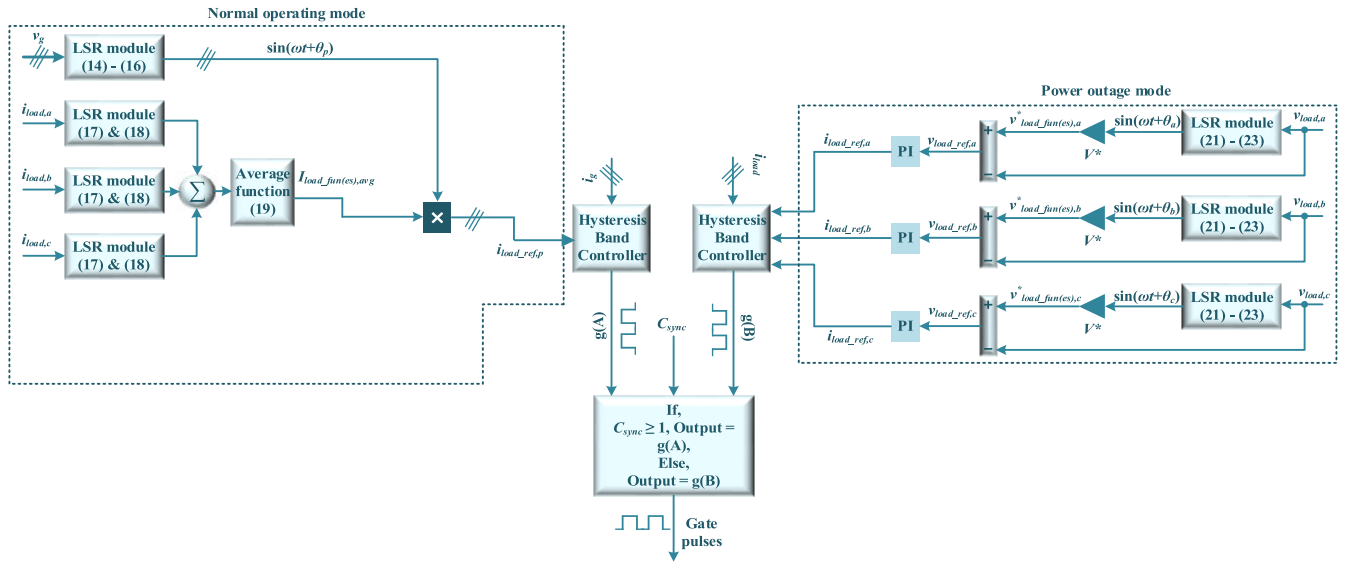where p indicates the phases of the system.

FIGURE 7. Unified LSR-based algorithm for P-INV.

Later, the averaging function of the mean magnitude ($I_{load\_fun(es)}$) is done to remove the ripples from the signals and can be formulated as:

$$I_{load\_fun(es),avg} = \frac{1}{3T_S} \int_0^{T_S} (I_{load\_fun(es),a}$$
$$+ I_{load\_fun(es),b}$$
$$+ I_{load\_fun(es),c})dt \quad (19)$$

where T_s indicates the system sample time. The reference current needs to be in phase with the grid voltage phase. One LSR module is utilized for synchronization which is discussed in section III-A.

To produce the reference current ($i_{load\_ref,p}$) accurately, the averaging function of mean magnitude ($I_{load\_fun(es),avg}$)) is multiplied by the synchronization function $\sin(\omega t + \theta_p)$. The hysteresis current controller receives the reference currents and produces the gating signals for the P-INV.

$$i_{load\_ref,p} = I_{load\_fun(es),avg} \times \sin(\omega t + \theta_p) \quad (20)$$

3) LSR-BASED POWER OUTAGE COMPENSATION

In the power outage mode, P-INV performs the voltage compensation to keep the load voltage at a desired phase and magnitude. In this case, the voltage information is taken from the load voltage (v_{load}). The extracted magnitude ($V_{load\_fun(es)}$) of the fundamental load voltage component ($v_{load\_fun(es)}$) is divided by the load voltage (v_{load}) to extract the sine function ($\sin(\omega t + \theta_p)$) in (23). The sine function is generated for the power outage mode and multiplied with the reference magnitude (V^*) in (24). Then the load current reference (i_{load_ref}) is achieved in (26). The expressions can be formulated as follows:

$$v_{load\_fun(es),p} = W_{1s}\sin(\omega t) + W_{1c}\cos(\omega t) \quad (21)$$

$$V_{load\_fun(es),p} = \sqrt{W_{1s}^2 + W_{1c}^2} \quad (22)$$

$$\sin(\omega t + \theta_p) = \frac{v_{load,p}}{V_{load\_fun(es),p}} \quad (23)$$

$$v_{load\_fun(es),p}^* = V^* \times \sin(\omega t + \theta_p) \quad (24)$$

$$v_{load\_ref,p} = v_{load\_fun(es),p}^* - v_{load,p} \quad (25)$$

$$i_{load\_ref,p} = K_{p(VD)}v_{Lref,x} + K_{i(VD)} \int_0^t v_{load\_ref,p}dt \quad (26)$$

The hysteresis current controller receives the reference currents for the normal operating mode or the power outage mode and produces the gating signals for P-INV. The control circuit for power outage detection decides the operating mode of the system which is either normal operating mode or power outage mode. The control diagram is simplified and presented in a flowchart, which can be seen in Fig. 8.

IV. RESULTS AND DISCUSSION

A fuel cell with a capacity of 6 kW is utilized, and the MATLAB Simulink environment is used to analyze the P-INV-FC system's dynamic behavior. To account for reactive power and harmonic removal in the event of non-linear loads, the developed network and techniques are evaluated and utilized under different circumstances. To assess the effectiveness of the suggested system, a grid-connected inverter with a $400V_{L-L}$ /50Hz setting is connected to the 6-kW fuel cell. The fuel cell's characteristic waveforms are illustrated in Fig. 4, which demonstrates that with a nominal output of 6 kW, voltage and current parameters for the fuel cell are 45 V and 133.3 A, respectively.

A thorough comparison with the traditional PQ control approach is used to demonstrate and further confirm the performance study of the proposed P-INV-FC system. There
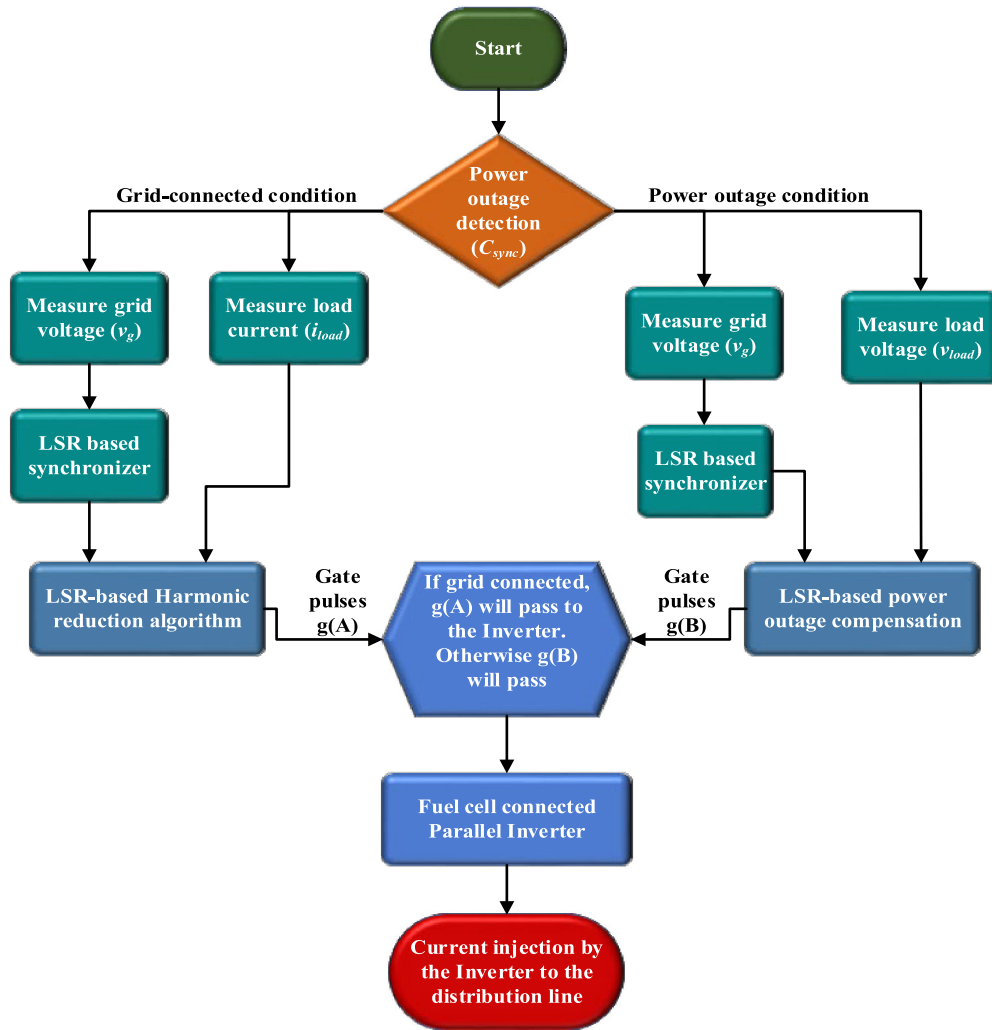
FIGURE 8. Flowchart of the Unified LSR-based algorithm for P-INV.

are two subcategories in the comparative assessment part depending on the simulation results. Firstly, the comparison between the proposed technique and the conventional PQ-controlled fuel-cell system or the PQFC system in terms of total harmonic distortions (THD) will be discussed. Secondly, the comparative assessment will be discussed with regard to power factor improvement.

A. PERFORMANCE OF P-INV DURING HARMONIC MITIGATION

To test the newly proposed unified LSR algorithm's capacity to reduce harmonics, extensive simulation tests are run utilizing three distinct grid voltages: standard utility voltage, imbalanced utility voltage, and harmonic-distorted utility voltage. A non-linear R-L load (50Ω-50 mH) (three-phase) is fed using the fuel-cell connected utility network. The specifications for the grid voltages that are being used are as follows:

Scenario 1: Grid voltage during nominal situations:

$$v_{g,a} = 326 \sin(\omega t) \tag{27}$$

$$v_{g,b} = 326 \sin(\omega t - 120°) \tag{28}$$

$$v_{g,c} = 326 \sin(\omega t + 120°) \tag{29}$$

Scenario 2: Grid voltage during imbalanced situations:

$$v_{g,a} = 220 \sin(\omega t) \tag{30}$$

$$v_{g,b} = 326 \sin(\omega t - 120°) \tag{31}$$

$$v_{g,c} = 270 \sin(\omega t + 120°) \tag{32}$$

Scenario 3: Grid voltage during distorted situations:

$$v_{g,a} = 326 \sin(\omega t) + 40 \sin(3\omega t) + 20 \sin(5\omega t)$$
$$+ 20 \sin(7\omega t) + 5 \sin(11\omega t) \tag{33}$$

$$v_{g,b} = 326 \sin(\omega t - 120°) + 40 \sin(3\omega t)$$
$$+ 20 \sin(5\omega t - 240°) + 20 \sin(7\omega t - 120°)$$
$$+ 5 \sin(11\omega t) \tag{34}$$

$$v_{g,c} = 326 \sin(\omega t + 120°) + 40 \sin(3\omega t)$$

TABLE 5. Grid current THD for three different grid voltage scenarios with unified LSR-based P-INV-FC and PQFC control.

Supply voltage scenario	THD (%) of supply current for several phases								
	Without compensator			With Unified LSR-P-INV-FC			With PQFC		
	Phase a	Phase b	Phase c	Phase a	Phase b	Phase c	Phase a	Phase b	Phase c
Scenario 1	27.84	27.84	27.84	0.75	0.78	0.76	3.23	3.28	3.26
Scenario 2	30.70	29.50	28.26	2.51	2.53	2.50	7.72	7.75	7.73
Scenario 3	28.18	28.18	28.18	1.39	1.40	1.42	5.89	5.92	5.91

$$+ 20 \sin\left(5\omega t + 240°\right) + 20 \sin\left(7\omega t + 120°\right)$$
$$+ 5 \sin\left(11\omega t\right) \tag{35}$$

The primary performance metric used to assess how well the proposed unified LSR algorithm performs is the THD score of mitigated source current, which has to be maintained under the 5% cap set by the IEEE 519 specification. In scenario 1, the proposed system's performance is compared to traditional PQ control in a balanced and distortion-free environment. The performance waveforms are illustrated in Fig. 9 in terms of the THD score of the grid current. Under typical circumstances, both algorithms appear to have operated as intended and have maintained the grid current's THD below 5% in accordance with IEEE 519 standards. Additionally, Table 5 shows that the suggested method

lowered the percentage of THD of source current (phase a) from 27.84% to 0.75%, whereas the traditional PQ reduced it from 27.84% to 3.23%. Fig. 10 displays the simulated waveforms related to Scenario 2. It is evident that the PQ algorithm performs unsatisfactorily when the grid voltage is unbalanced (Scenario 2). With the PQ method, THD scores of supply currents are reduced from 30.70% to 7.72%, as illustrated in Fig. 10 (d) and reported in Table 5. However, it has been shown that the recommended unified LSR algorithm performs better than the PQ method when the grid voltage is unbalanced. Only around 2.51% of the THD value was recorded with unified LSR as presented in Table 5. Furthermore, under harmonically distorted (Scenario 3) grid voltage settings, the PQ method once more failed to yield results that were not satisfactory. Fig. 11 shows the simulated waveforms for this Scenario 3 and according to Table 5, the PQ method utilized the system produced supply current with the THD scores of 5.89%, which is in violation of IEEE specifications. Conversely, the unified LSR algorithm effectively complies with IEEE 519 specifications and reduces THD values to around 1.39%. Since the non-linear load was the only source of THD injection during Scenario 1, the PQ algorithm was able to successfully attenuate the harmonics with the help of the LPF. However, in Scenario 2, the PQ method is unable to mitigate the supply current. The PQ method is not capable of regulating the supply voltage fluctuations due to the absence of a phase estimator, which ultimately caused the supply current to exhibit large ripple quantities and phase disruptions. But in Scenario 3, the utility and the non-linear load introduced distortions into the network, the overall THD is increased in comparison with Scenario 1. As a result, in Scenario 3, the LPF was unable to lower the THD below

the standard due to its weak filtration capabilities, as it lacks a phase estimator like PLL. Although some of the work use PLL in the PQ method [49], however, the result is not satisfactory.

B. PERFORMANCE OF P-INV DURING A POWER OUTAGE
In this section, the power outage mode is investigated and considered as scenario 4. The performance of the unified LSR-based P-INV-FC in the course of transition is depicted in Fig. 12. It can be seen from Fig. 12 that when the grid is disconnected due to fault conditions at 0.8 seconds, the load voltage was maintained by P-INV. The sustainable energy management system conductor switches are activated once all the conditions of grid activation are met ($C_{sync} = 1$), and the P-INV starts performing in the normal operating mode. The power outage detection method was discussed in the section III-B-I. The maintained load voltage at the rated value is shown in Fig. 12 (b) regardless of the power outage. Depending on the control circuit of the power outage detection output, the P-INV-FC system starts supporting the critical loads during the power outage situation. On the other hand, the PQFC system is unable to support the critical loads during a power outage situation as it does not have any control circuit to detect the power outage and also does not incorporate any control algorithm to compensate for the power outage.

C. ANALYSIS OF POWER FACTOR CORRECTION
By supplying parallel-connected (R-L) loads to the utility network, the suggested system's capacity to rectify the power factor is examined. When t is between 0.0-0.8 s and (R = 55, L = 36 mH) is chosen for load 1 is operating, the system is in the first mode. At t = 0.8 s, mode 2 takes over the proposed configuration's functioning. In this case, R = 35, L = 55 mH) is chosen for load 2 connected to the utility network but load 1 is disconnected. Load 2 is turned off and (R = 45, L = 40 mH) is engaged as load 3 in mode 3. Fig. 13 shows the fuel-cell-connected utility network's active/reactive power flow data for three distinct R-L loads. As shown in Fig. 13(a) and Fig. 13(b), both the proposed and conventional network deliver equivalent active powers from the fuel cell, load, and utility grid. For the grid network's R-L loads, the fuel cell facility supplies around 6 kW of electricity. The loads, however, use active powers of 8 kW for mode 1, during mode 2, the load consumes 9.9 kW, and during mode 3 the load consumes 8.7 kW. Consequently, the utility network provides power to the loads which are 2 kW in the course of mode 1, in the course of mode 2, it provides 3.9 kW,
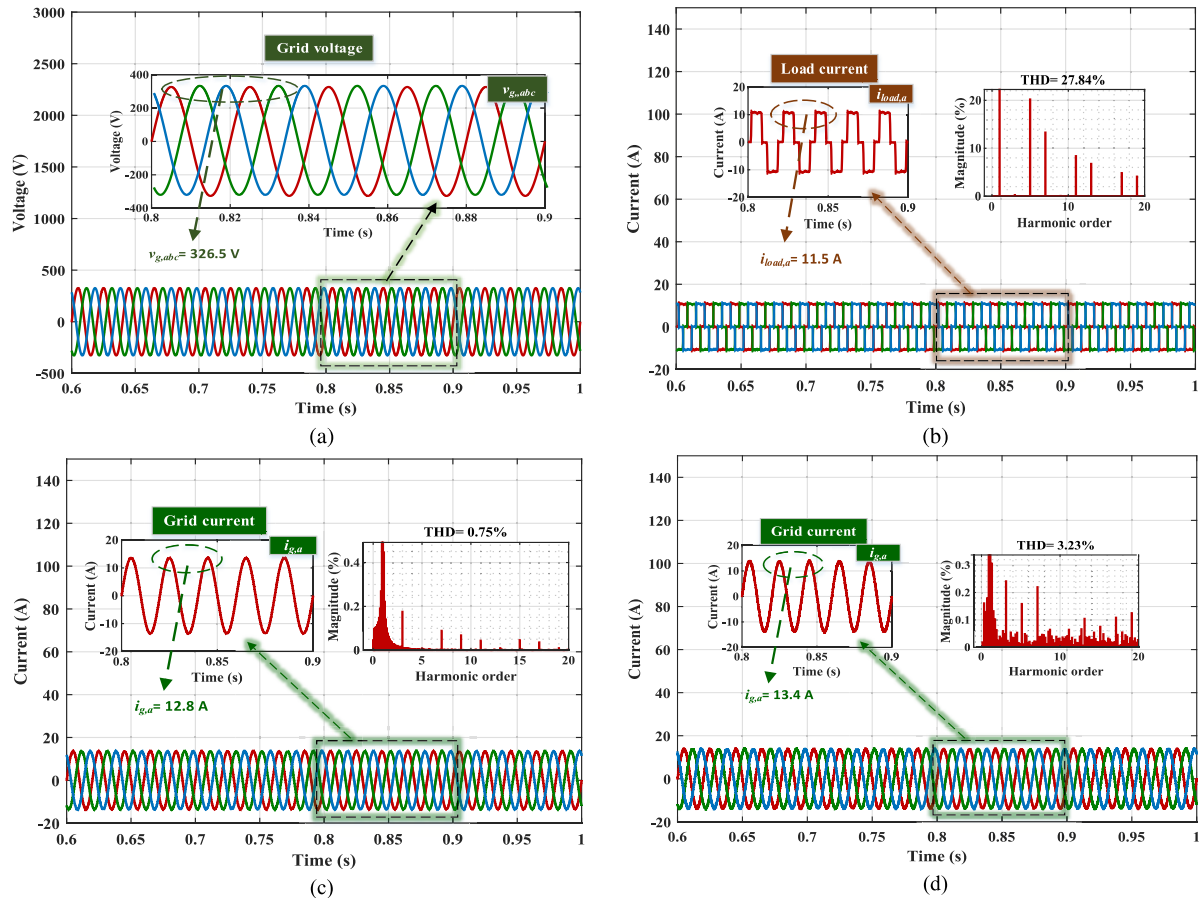
FIGURE 9. Performance evaluation during scenario 1 in between proposed unified LSR-based P-INV-FC versus the traditional PQFC (a) Grid voltage (v_g) (b) Load current (i_{load}) (c) Grid current (i_g) for P-INV-FC (d) Grid current (i_g) for PQFC.

TABLE 6. Statistics of reactive power for three different (R-L) loads with unified LSR and PQ method.

	Mode 1			Mode 2			Mode 3		
Period of time	0s < t < 0.8s			0.8s < t < 1.6s			1.6s < t < 2.4s		
Loads	R = 55 Ω, L = 36 mH			R = 35 Ω, L = 55 mH			R = 45 Ω, L = 40 mH		
	Reactive power								
	Unified LSR			PQ method					
	Mode 1 (kVAR)	Mode 2(kVAR)	Mode 3(kVAR)	Mode 1(kVAR)	Mode 2(kVAR)	Mode 3(kVAR)			
Utility-Grid	0.008	0.012	0.012	0.82	2.1	1.1			
Fuel-cell	0.82	2.10	1.0	0.0	0.0	0.0			
Load	0.82	2.10	1.0	0.82	2.1	1.1			

and in the course of mode 3, it delivers 2.7 kW. Reactive power is a situation when the conventional strategy falls short of compensating for reactive power, resulting in the inductive load drawing the whole reactive power supplied by the utility network. According to Fig. 13 (c), the load receives reactive power in the course of mode 1 is 0.82 kVAR, in the course of mode 2, it receives 2.1 kVAR, and in the course of mode 3, it receives 1 kVAR for the proposed P-INV-FC system. Conversely, for traditional PQFC management, the reactive measurement in the load recorded in the course of mode 1 is 0.82 kVAR, in the course of mode 2, it is 2.1 kVAR, and in the course of mode 3, it is 1.1 kVAR., which result in a rise in perceived power. On the performance outcomes, Table 6 gives specific information. The performance findings show that the proposed unified LSR-based P-INV-FC system effectively

prevents reactive power transfer from the power system while yet providing vital reactive power by the fuel cell toward the loads. According to the results, deploying a fuel cell to deliver large reactive power for the utility grid is not possible utilizing the traditional PQFC system. As demonstrated in Fig. 13 (d), the fuel-cell unit provides nearly no reactive power to the load in the conventional PQ fuel-cell system. However, in the suggested technique-based P-INV-FC system, the fuel cell can provide 0.82 kVAR reactive power for load 1, for load 2, it can provide 2.10 kVAR, and for load 3, it can provide 1.0 kVAR. The unified LSR regulation thus decreased the reactive power quantity delivered by the utility. The results indicate that in real-world circumstances, the unified LSR-based SEM system is capable of reducing the power demand that is supposed to supply by the utility network and prevent
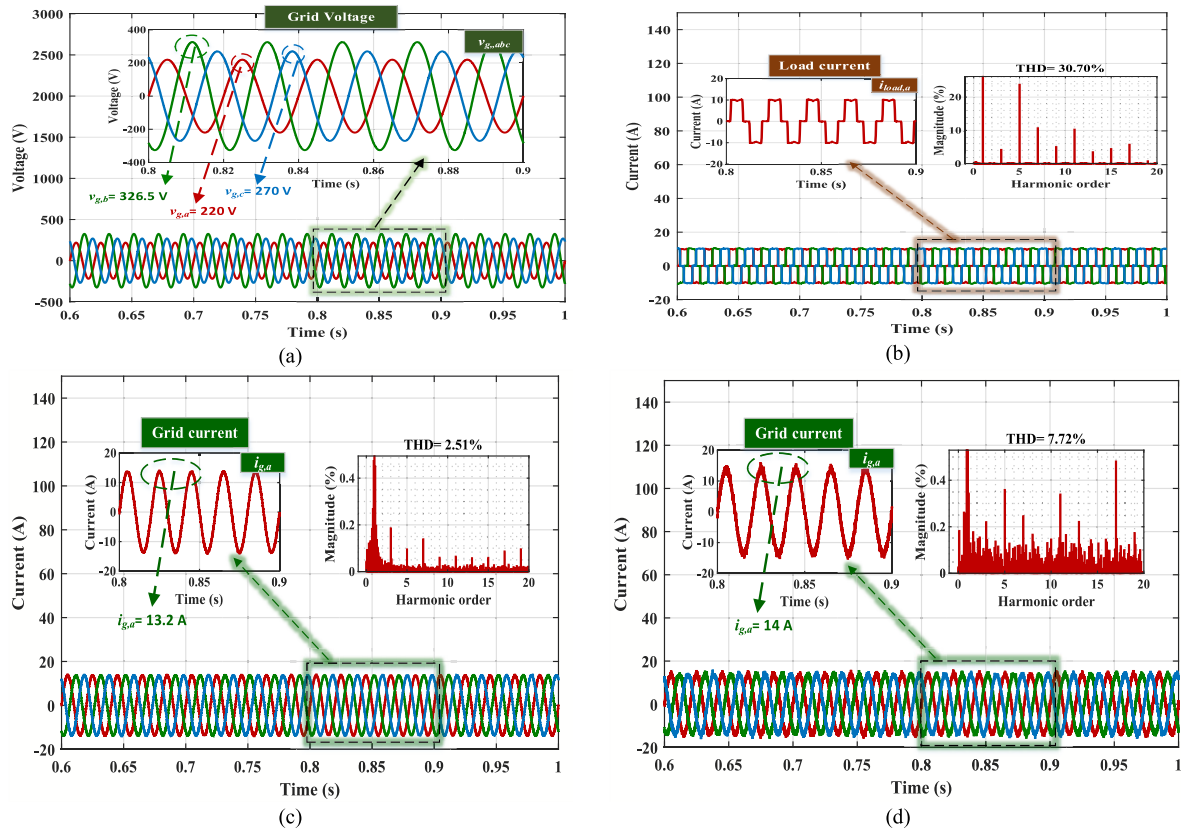
FIGURE 10. Performance evaluation during scenario 2 in between proposed unified LSR-based P-INV-FC versus the traditional PQFC (a) Grid voltage (v_g) (b) Load current (i_{load}) (c) Grid current (i_g) for P-INV-FC (d) Grid current (i_g) for PQFC.

TABLE 7. Power factors utilizing three (R-L) loads for unified LSR-based P-INV-FC and PQFC system.

Unified LSR control	PQ control
0.99	0.89
0.99	0.81
0.99	0.87

excessive fines for consumers. For measured local inductive loads, power factor values are far below the necessary levels without reactive power adjustment.

For both the proposed system and the traditional PQFC system, the power factor scores utilizing distinct loads are illustrated in Fig. 14. For the PQFC system, in three different modes, the power factor is recorded, and they are 0.89, 0.81, and 0.87. Conversely, a power factor of 1 is observed when the proposed system is utilized to keep track of how reactive power is transferred in the middle of the utility network and loads. Additionally, Table 7 shows the power factors for the proposed system versus the traditional PQFC system.

The findings of Fig. 14 make it clear that the standard PQ control was unable to use the fuel cell unit's reactive power in order to meet the requirement of load transients. Because of this, the grid was providing all of the load's reactive power requirements, which led to a decline in the system's power factor (as shown in Fig. 14 (b)) and a violation of the US Department of Energy regulation. A bulky conductor, excessive loss of copper, poorly controlled voltage, and higher kVA-rated components, are just a few examples of how power

factor degradation may negatively affect the whole system. These effects have a significant negative influence on a grid system's overall effectiveness and efficiency. Additionally, Fig. 14 shows that when the PQFC system is used and the load value is altered, the power factor changes. This abrupt shift in power factor has the potential to seriously harm the fuel cell unit. On the other hand, the proposed system, as illustrated in Fig. 13 (c) and 14 (a), has effectively corrected the system's power factor by providing the load with the required reactive power using the fuel cell unit. Additionally, it maintained the system's power factor at a steady level throughout load fluctuations. In contrast to traditional PQFC system regulation, it has effectively prevented any adverse consequences. related to power factor degradation and variance.

D. COMPARATIVE ANALYSIS WITH OTHER SEMS FOR FUEL-CELL CONNECTED UTILITY NETWORK

A short comparison analysis is presented in this part and provided in Table 8 in order to further support the benefit of the proposed system. The comparison is made using five different criteria, including the reduction of THD in the four case studies covered in the previous sections IV-A and IV-B, the type of SEM used in synchronization strategy, power outage performance, and the complexity of the system. The comparison demonstrates that the proposed unified LSR-based P-INV-FC SEM has outperformed the other recently proposed FC SEMs in terms of THD reduction. The FC
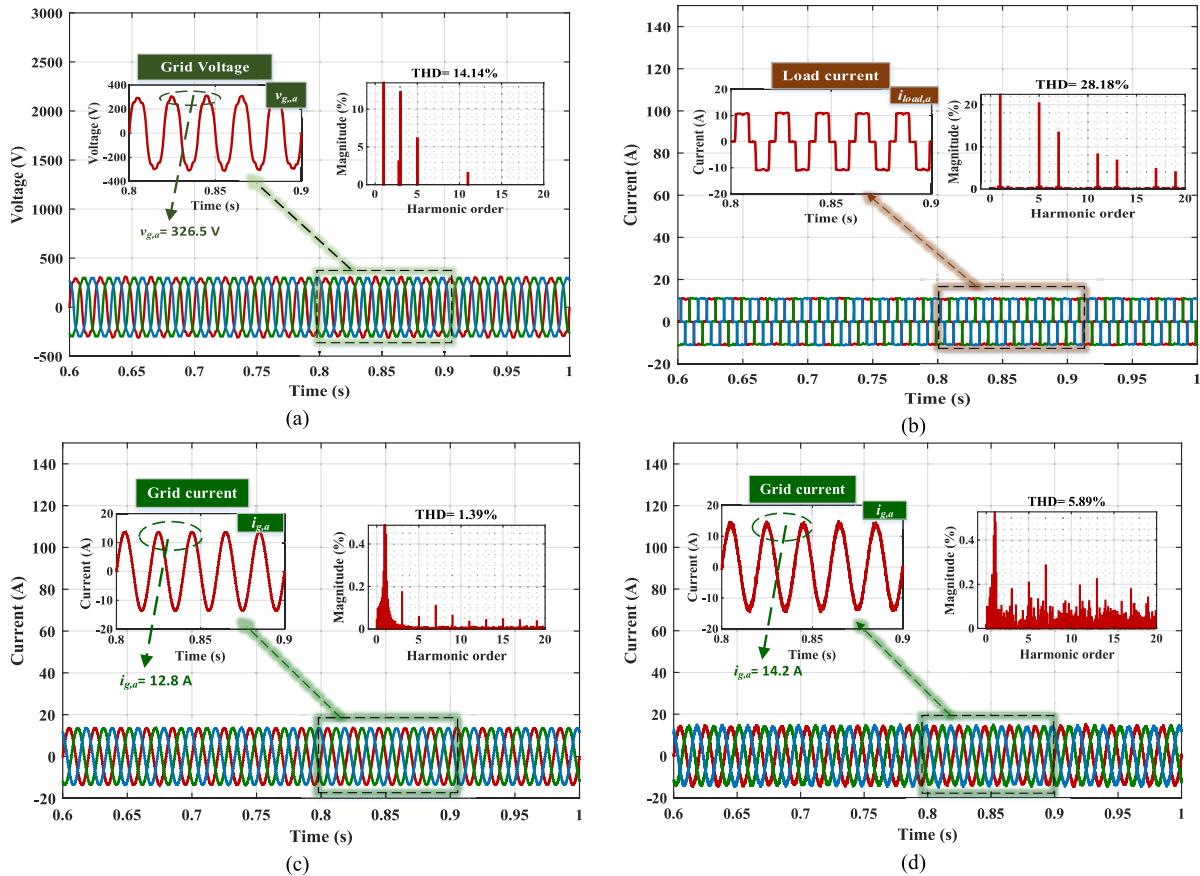
FIGURE 11. Performance evaluation during scenario 3 in between proposed unified LSR-based P-INV-FC versus the traditional PQFC (a)Grid voltage (v_g) (b) Load current (i_{load}) (c) Grid current (i_g) for P-INV-FC (d) Grid current (i_g) for PQFC.
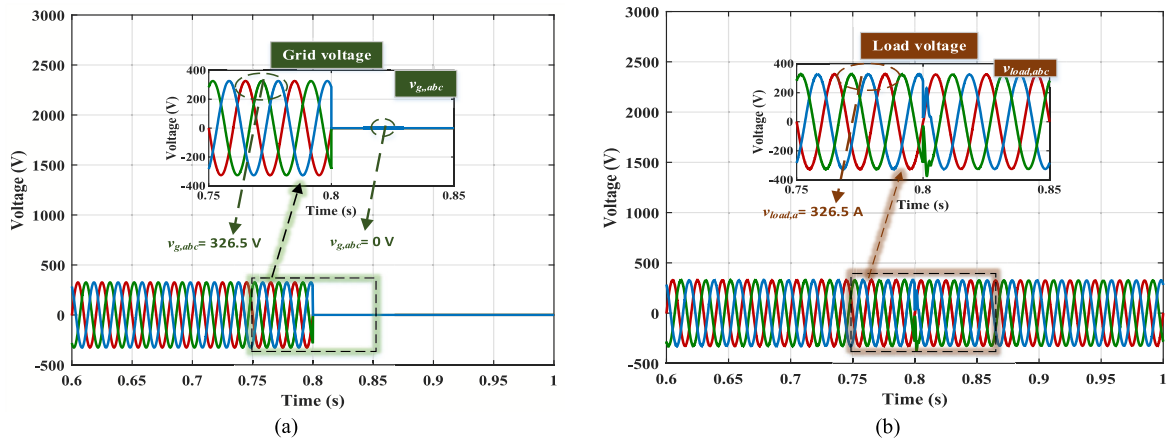

FIGURE 12. Performance evaluation during scenario 4 in between the proposed unified LSR-based P-INV-FC versus the traditional PQFC (a)Grid voltage (v_g) (b) Load voltage (v_{load}).

SEM suggested in [38] has the closest performance. However, compared to the other FC system in this comparison, this system is the most costly and complicated due to the usage of 25-level CHB MLI, which requires 12 independent DC sources and transformers. Most of the FC systems utilized conventional PLL for synchronization purposes which has many shortcomings during grid voltage oddity such as phase delay, unable to remove the harmonic component, and so on. However, [38] and [50] utilized PID, and Kalman and fuzzy integrated controllers, respectively, for synchronization purposes. Nonetheless, Kalman and fuzzy integrated controllers introduce a higher computation burden and make the overall SEM complex. In terms of power outage performance which is a very important scenario, especially for the critical load condition, only one of the studies [38] considered 20% voltage reduction and increase, however, the power outage performance is not covered on any FC SEMs.
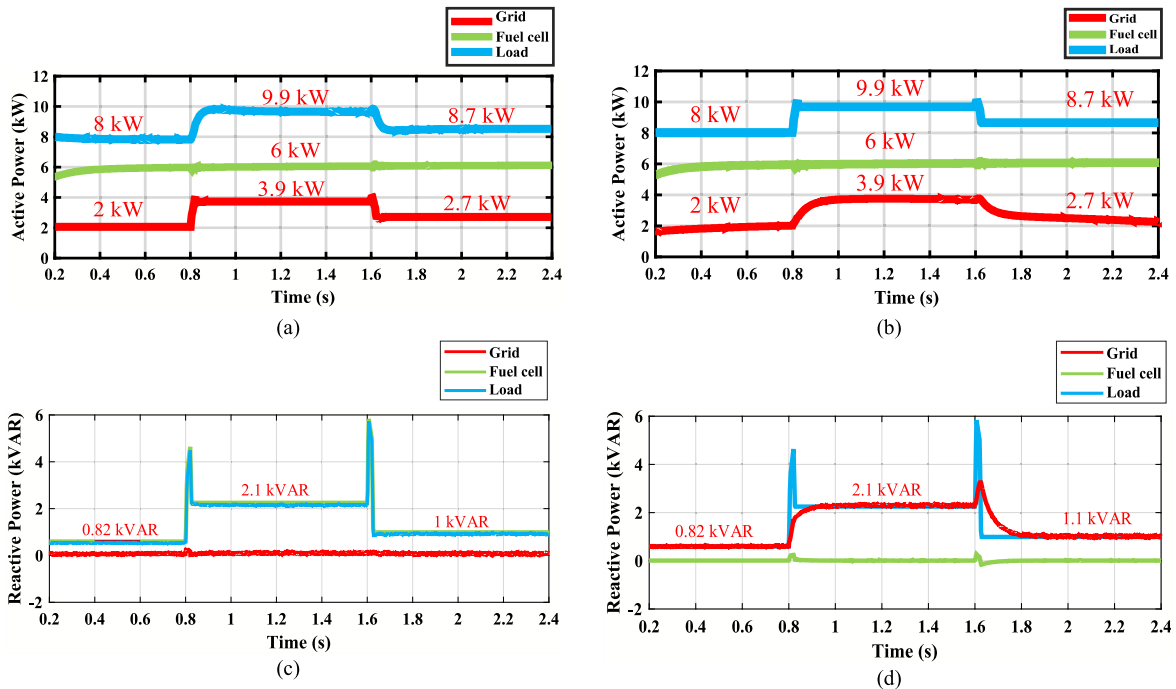
FIGURE 13. Power flow analysis of the proposed unified LSR-based P-INV-FC and PQFC under load-changing mode: (a) active power for proposed system (b) active power for PQFC (c) reactive power for proposed system (d) reactive power for PQFC.
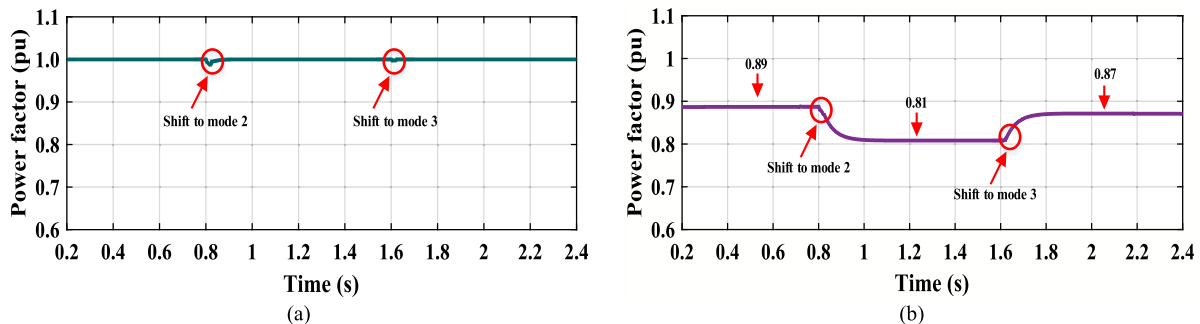

FIGURE 14. Regulation of power factor for three inductive loads for (a) unified LSR control and (b) PQ control.

TABLE 8. Comparative analysis between various recently proposed FC SEMs.

FC SEMs	THD Mitigation			SEM	Synchronizer	Power Outage Performance (Case 4)	Complexity
	Case 1	Case 2	Case 3				
[29]	1.59%	4.15%	3.25.%	DQ with PLL	Conventional PLL	Not possible	Simple
[24]	2.94%	6.15%	4.12%	V-PI	Conventional PLL	Not possible	Complex
[17]	1.71%	4.25%	3.36%	DQ with PLL	Conventional PLL	Not possible	Simple
[22]	2.67%	5.86%	3.88%	DQ with PLL	Conventional PLL	Not possible	Simple
[38]	0.44%	2.84%	2.92%	ISSA-PID	PID	Moderate	Complex
[49]	3.51%	8.82%	5.78%	PQ with PLL	Conventional PLL	Not possible	Complex
[50]	3.19%	3.68%	3.96%	PEKF	Kalman and Fuzzy	Not possible	Complex
Proposed	0.75.%	2.51%	1.39%	Unified LSR	LSR	Solved	Simple

V. CONCLUSION

In this article, an enhanced control for a fuel-cell connected utility network called a unified linear self-regulating (LSR)-based sustainable energy management system (SEM) is presented based on an active/reactive SEM. The benefit and viability of the unified LSR SEM system are proven by comparative assessment and a series of scenarios in relation to the traditional PQ method and other FC SEMs. The following statements serve as a summary of the conclusions.

- The standard PLL's dynamic response is contrasted with that of the LSR employed in the proposed network. The PLL's dynamic reaction is extremely slow and contains unnecessary overshoots, while the dynamic response of the LSR is always constant at 50 Hz after it becomes stable, regardless of the presence of harmonics. This was shown by a thorough investigation. This comparative investigation demonstrated that fuel-cell connected utility networks employing

traditional PLL lack the dynamic responsiveness and filtering capabilities required to fulfill IEEE standards and industry requirements. The suggested LSR successfully enhanced the fuel-cell-connected utility network's performance in accordance with industry benchmarks and requirements.

- Three case studies were used to analyze and compare the performance of the proposed system and traditional PQFC employing non-linear loads. The proposed system has consistently outperformed the PQFC system in every situation. The grid current generated by PQ control integrated fuel cells in scenarios 2 and 3 has a high THD of 7.72% and 5.89%, respectively, and does not comply with IEEE 519 standards. LPF's use is the cause of the poor PQ control outcomes. However, when the suggested unified LSR control was used, the THD of the supply current is only decreased to 2.51% and 1.39%, which is much below the necessary level that is THD ≤ 5% established by IEEE standard 519. Since the unified LSR has stronger filtering capabilities than conventional LPF, the unified LSR control had better results. These findings show that the unified LSR control has been incorporated into the fuel-cell-connected utility network, making it appropriate for industry solutions.

- The proposed SEM consists of a power outage detection circuit that can detect power outage situations and can support critical loads using fuel-cell power. None of the literature was found to solve this significant power quality issue other than a few SEMs which are considered a small percentage of voltage sag/swell.

- In addition, the suggested unified LSR control and PQ control's capacity to rectify power factor is analyzed and compared under three load-varying scenarios. Noticeably, the fuel cell is not capable of providing reactive power to the load in the PQFC system. Therefore, the power factor is degraded and recorded as 0.89 for PQFC in the course of mode 1, and in the course of mode 2, it is 0.81, and in the course of mode 3, it is 0.87. The proposed SEM, on the other hand, enables efficient management of reactive power betwixt the loads and the fuel cell. As a consequence, a constant power factor is maintained throughout the operation under all load situations. As a result, the suggested system complies with the US Department of Energy's Energy Star criteria that the power factor should be greater or equal to 0.95. This further validated the suggested SEM's industrial applicability.

- Grid current's THD spectrum is contrasted with those of other newly produced FC SEMs to show the variations in their harmonic reduction capacities. When compared to other FC SEMs with comparable characteristics, the comparison also showed that the proposed SEM is better in terms of performance, as well as simple in terms of control.

REFERENCES

[1] M. Inci and Ö. Türksoy, "Review of fuel cells to grid interface: Configurations, technical challenges and trends," *J. Cleaner Prod.*, vol. 213, pp. 1353–1370, Mar. 2019.

[2] V. Das, S. Padmanaban, K. Venkitusamy, R. Selvamuthukumaran, F. Blaabjerg, and P. Siano, "Recent advances and challenges of fuel cell based power system architectures and control—A review," *Renew. Sustain. Energy Rev.*, vol. 73, pp. 10–18, Jun. 2017.

[3] N. Sulaiman, M. A. Hannan, A. Mohamed, P. J. Ker, E. H. Majlan, and W. R. Wan Daud, "Optimization of energy management system for fuel-cell hybrid electric vehicles: Issues and recommendations," *Appl. Energy*, vol. 228, pp. 2061–2079, Oct. 2018.

[4] M. Gharibi and A. Askarzadeh, "Size and power exchange optimization of a grid-connected diesel generator-photovoltaic-fuel cell hybrid energy system considering reliability, cost and renewability," *Int. J. Hydrogen Energy*, vol. 44, no. 47, pp. 25428–25441, Oct. 2019.

[5] R. Guo, Q. Li, and N. Zhao, "An overview of grid-connected fuel cell system for grid support," *Energy Rep.*, vol. 8, pp. 884–892, Nov. 2022.

[6] R. Hemmati and H. Faraji, "Identification of cyber-attack/outage/fault in zero-energy building with load and energy management strategies," *J. Energy Storage*, vol. 50, Jun. 2022, Art. no. 104290.

[7] R. Rodriguez, G. Osma, D. Bouquain, J. Solano, G. Ordoñez, R. Roche, D. Paire, and D. Hissel, "Sizing of a fuel cell–battery backup system for a university building based on the probability of the power outages length," *Energy Rep.*, vol. 8, pp. 708–722, Nov. 2022.

[8] L. Sun, Y. Jin, L. Pan, J. Shen, and K. Y. Lee, "Efficiency analysis and control of a grid-connected PEM fuel cell in distributed generation," *Energy Convers. Manage.*, vol. 195, pp. 587–596, Sep. 2019.

[9] E. Hossain, M. R. Tür, S. Padmanaban, S. Ay, and I. Khan, "Analysis and mitigation of power quality issues in distributed generation systems using custom power devices," *IEEE Access*, vol. 6, pp. 16816–16833, 2018.

[10] Y. Luo, Y. Wu, B. Li, T. Mo, Y. Li, S.-P. Feng, J. Qu, and P. K. Chu, "Development and application of fuel cells in the automobile industry," *J. Energy Storage*, vol. 42, Oct. 2021, Art. no. 103124.

[11] M. Inci, "Future vision of hydrogen fuel cells: A statistical review and research on applications, socio-economic impacts and forecasting prospects," *Sustain. Energy Technol. Assessments*, vol. 53, Oct. 2022, Art. no. 102739.

[12] A. G. Olabi, T. Wilberforce, and M. A. Abdelkareem, "Fuel cell application in the automotive industry and future perspective," *Energy*, vol. 214, Jan. 2021, Art. no. 118955.

[13] M. S. Okundamiya, "Size optimization of a hybrid photovoltaic/fuel cell grid connected power system including hydrogen storage," *Int. J. Hydrogen Energy*, vol. 46, no. 59, pp. 30539–30546, Aug. 2021.

[14] Y. Hoon, M. M. Radzi, M. Hassan, and N. Mailah, "Control algorithms of shunt active power filter for harmonics mitigation: A review," *Energies*, vol. 10, no. 12, p. 2038, Dec. 2017.

[15] *Energy Star? Program Requirements for Single Voltage External AC-DC and AC-AC Power Supplies Eligibility Criteria (Version 2.0) Final Table of Contents*, Energy Star, Charlotte, NC, USA, 2008.

[16] *IEEE Recommended Practice and Requirements for Harmonic Control in Electric Power Systems*, IEEE Power Energy Soc., Piscataway, NJ, USA, 2014.

[17] H. A. Azzeddine, D. E. Chaouch, M. Berka, M. Hebali, A. L. Hebali, and M. Tioursi, "Fuel cell grid connected system with active power generation and reactive power compensation features," *Przegląd Elektrotechniczny*, vol. 96, no. 11, pp. 124–127, 2020.

[18] A. Mojallal and S. Lotfifard, "Improving during and postfault response of fuel cells in symmetrical and asymmetrical grid fault cases," *IEEE Trans. Sustain. Energy*, vol. 9, no. 3, pp. 1407–1418, Jul. 2018.

[19] Y. Zhu, H. Wang, and Z. Zhu, "Improved VSG control strategy based on the combined power generation system with hydrogen fuel cells and super capacitors," *Energy Rep.*, vol. 7, pp. 6820–6832, Nov. 2021.

[20] Y. Hoon and M. M. Radzi, "PLL-less three-phase four-wire SAPF with STF-*dq*0 technique for harmonics mitigation under distorted supply voltage and unbalanced load conditions," *Energies*, vol. 11, no. 8, p. 2143, Aug. 2018.

[21] K. Hasan S. T. Meraj, M. M. Othman, M. S. H. Lipu, M. A. Hannan, and K. M. Muttaqi, "Savitzky–Golay filter-based PLL: Modeling and performance validation," *IEEE Trans. Instrum. Meas.*, vol. 71, 2022, Art. no. 2004306.

[22] M. Priya and P. Ponnambalam, "Three-phase grid connected modular-multilevel converter fed by proton exchange membrane fuel cell," *Int. J. Renew. Energy Res.*, vol. 12, no. 1, pp. 466–478, Mar. 2022.

[23] M. Aguirre, H. Couto, and M. I. Valla, "Analysis and simulation of a hydrogen based electric system to improve power quality in distributed grids," *Int. J. Hydrogen Energy*, vol. 37, no. 19, pp. 14959–14965, Oct. 2012.

[24] Q. Li, W. Chen, Z. Liu, G. Zhou, and L. Ma, "Active control strategy based on vector-proportion integration controller for proton exchange membrane fuel cell grid-connected system," *IET Renew. Power Gener.*, vol. 9, no. 8, pp. 991–999, Nov. 2015.

[25] M. I. Mosaad and H. S. Ramadan, "Power quality enhancement of grid-connected fuel cell using evolutionary computing techniques," *Int. J. Hydrogen*, vol. 43, no. 25, pp. 11568–11582, Jun. 2018.

[26] Q. Li, X. Meng, F. Gao, G. Zhang, W. Chen, and K. Rajashekara, "Reinforcement learning energy management for fuel cell hybrid system: A review," *IEEE Ind. Electron. Mag.*, early access, Feb. 21, 2022, doi: 10.1109/MIE.2022.3148568.

[27] Q. Li, X. Meng, F. Gao, G. Zhang, and W. Chen, "Approximate cost-optimal energy management of hydrogen electric multiple unit trains using double *Q*-learning algorithm," *IEEE Trans. Ind. Electron.*, vol. 69, no. 9, pp. 9099–9110, Sep. 2022.

[28] L. Sun, G. Wu, Y. Xue, J. Shen, D. Li, and K. Y. Lee, "Coordinated control strategies for fuel cell power plant in a microgrid," *IEEE Trans. Energy Convers.*, vol. 33, no. 1, pp. 1–9, Mar. 2018.

[29] W. Chen, Y. Han, Q. Li, Z. Liu, and F. Peng, "Design of proton exchange membrane fuel cell grid-connected system based on resonant current controller," *Int. J. Hydrogen Energy*, vol. 39, no. 26, pp. 14402–14410, Sep. 2014.

[30] A. K. Roy, P. Basak, and G. R. Biswal, "Low voltage ride through capability enhancement in a grid-connected wind/fuel cell hybrid system via combined feed-forward and fuzzy logic control," *IET Gener., Transmiss. Distrib.*, vol. 13, no. 13, pp. 2866–2876, Jul. 2019.

[31] Y. Bicer, I. Dincer, and M. Aydin, "Maximizing performance of fuel cell using artificial neural network approach for smart grid applications," *Energy*, vol. 116, pp. 1205–1217, Dec. 2016.

[32] G. Bayrak and M. Cebeci, "Grid connected fuel cell and PV hybrid power generating system design with MATLAB simulink," *Int. J. Hydrogen Energy*, vol. 39, no. 16, pp. 8803–8812, May 2014.

[33] S. K. Ayyappa and D. N. Gaonkar, "Performance analysis of a variable-speed wind and fuel cell-based hybrid distributed generation system in grid-connected mode of operation," *Electr. Power Compon. Syst.*, vol. 44, no. 2, pp. 142–151, Jan. 2016, doi: 10.1080/15325008.2015.1102988.

[34] A. Sabir, "A PLL-free robust control scheme with application to grid-connected fuel cell DGs under balanced and unbalanced conditions," *Sustain. Energy Technol. Assessments*, vol. 31, pp. 64–76, Feb. 2019.

[35] M. İnci, "Active/reactive energy control scheme for grid-connected fuel cell system with local inductive loads," *Energy*, vol. 197, Apr. 2020, Art. no. 117191.

[36] G. Wu, L. Sun, and K. Y. Lee, "Disturbance rejection control of a fuel cell power plant in a grid-connected system," *Control Eng. Pract.*, vol. 60, pp. 183–192, Mar. 2017.

[37] Q. Li, P. Liu, X. Meng, G. Zhang, Y. Ai, and W. Chen, "Model prediction control-based energy management combining self-trending prediction and subset-searching algorithm for hydrogen electric multiple unit train," *IEEE Trans. Transport. Electrific.*, vol. 8, no. 2, pp. 2249–2260, Jun. 2022.

[38] S. Choudhury, S. K. Acharya, R. K. Khadanga, S. Mohanty, J. Arshad, A. U. Rehman, M. Shafiq, and J.-G. Choi, "Harmonic profile enhancement of grid connected fuel cell through cascaded H-bridge multi-level inverter and improved squirrel search optimization technique," *Energies*, vol. 14, no. 23, pp. 1–20, 2021.

[39] S. N. V. B. Rao, Y. V. P. Kumar, D. J. Pradeep, C. P. Reddy, A. Flah, H. Kraiem, and J. F. Al-Asad, "Power quality improvement in renewable-energy-based microgrid clusters using fuzzy space vector PWM controlled inverter," *Sustainability*, vol. 14, no. 8, p. 4663, Apr. 2022.

[40] S. N. V. B. Rao, Y. V. P. Kumar, M. Amir, and F. Ahmad, "An adaptive neuro-fuzzy control strategy for improved power quality in multi-microgrid clusters," *IEEE Access*, vol. 10, pp. 128007–128021, 2022.

[41] K. Hasan, M. M. Othman, N. F. A. Rahman, M. A. Hannan, and I. Musirin, "Significant implication of unified power quality conditioner in power quality problems mitigation," *Int. J. Power Electron. Drive Syst.*, vol. 10, no. 4, pp. 2231–2237, 2019.

[42] S. T. Meraj, N. Z. Yahaya, K. Hasan, M. S. Hossain Lipu, A. Masaoud, S. H. M. Ali, A. Hussain, M. M. Othman, and F. Mumtaz, "Three-phase six-level multilevel voltage source inverter: Modeling and experimental validation," *Micromachines*, vol. 12, no. 9, p. 1133, Sep. 2021.

[43] K. Hasan, M. M. Othman, S. T. Meraj, M. S. Rahman, M. S. H. Lipu, and P. Kotsampopoulos, "DC-AC converter with dynamic voltage restoring ability based on self-regulated phase estimator-DQ algorithm: Practical modeling and performance evaluation," *Electronics*, vol. 12, no. 3, p. 523, Jan. 2023.

[44] N. M. Souleman, O. Tremblay, and L.-A. Dessaint, "A generic fuel cell model for the simulation of fuel cell power systems," in *Proc. IEEE Power Energy Soc. Gen. Meeting*, vol. 9, Jul. 2009, pp. 1722–1729.

[45] M. V. Naik and P. Samuel, "Analysis of ripple current, power losses and high efficiency of DC–DC converters for fuel cell power generating systems," *Renew. Sustain. Energy Rev.*, vol. 59, pp. 1080–1088, Jun. 2016.

[46] M. E. Raoufat, A. Khayatian, and A. Mojallal, "Performance recovery of voltage source converters with application to grid-connected fuel cell DGs," *IEEE Trans. Smart Grid*, vol. 9, no. 2, pp. 1197–1204, Mar. 2018.

[47] M. Büyük, A. Tan, M. Tümay, and K. Ç. Bayindir, "Topologies, generalized designs, passive and active damping methods of switching ripple filters for voltage source inverter: A comprehensive review," *Renew. Sustain. Energy Rev.*, vol. 62, pp. 46–69, Sep. 2016.

[48] Y. Hoon, M. Hassan, N. Mailah, and M. M. Radzi, "A self-tuning filter-based adaptive linear neuron approach for operation of three-level inverter-based shunt active power filters under non-ideal source voltage conditions," *Energies*, vol. 10, no. 5, p. 667, May 2017.

[49] M. İnci, "Interline fuel cell (I-FC) system with dual-functional control capability," *Int. J. Hydrogen Energy*, vol. 45, no. 1, pp. 891–903, Jan. 2020.

[50] S. Gobimohan, "Active power quality improvement for unified renewable energy system with multilevel inverter and PEKF controllers," *Energy Sources A, Recovery, Utilization, Environ. Effects*, vol. 42, no. 21, pp. 2603–2622, Nov. 2020.

KAMRUL HASAN received the B.Sc. degree in electrical and electronics engineering from the Ahsanullah University of Science and Technology, Dhaka, Bangladesh, in 2015, and the M.Sc. degree in electrical engineering from Curtin University, Miri, Malaysia, in 2018. He is currently pursuing the Ph.D. degree with the School of Electrical Engineering, UiTM, Shah Alam, Malaysia.

Since March 2019, he has been a Graduate Research Assistant (GRA) on a research project titled "Power Quality Problems Mitigation in Energy Storage System (ESS)" under the Long Research Grant Scheme (LRGS) of the Ministry of Higher Education (MOHE), Malaysia. He is also a Postgraduate Teaching Assistance (UPTA) with UiTM. His research interests include power electronics, power quality, custom power devices, and renewable energy resources.

MUHAMMAD MURTADHA OTHMAN (Member, IEEE) received the B.Eng. degree (Hons.) from Staffordshire University, England, in 1998, the M.Sc. degree from Universiti Putra Malaysia, in 2000, and the Ph.D. degree from Universiti Kebangsaan Malaysia, in 2006. He was the former Director of the UiTM Solar Research Institute (SRI) Centre under the project of 50MW LSSPV at Gambang, Pahang. He was also the Head of the Department of the Centre for Electrical Power Engineering Studies (CEPES), from February 2009 to December 2010. He is currently an Associate Professor with the College of Engineering, Universiti Teknologi MARA (UiTM), Malaysia. Since 2012, he has been serving two times as the Deputy Director for the collaborative research project under the auspices of the Ministry of Energy, Green Technology and Water (KeTTHA), Malaysia, and the Public Works Department (JKR), Malaysia. He has over 20 years of research experience in energy demand/supply modeling particularly related to the field of power system operation and planning composed of electric power generation, transmission, and distribution. He has led several projects under the auspices of research grants sponsored by the government and industry. He is also working on a special research project task related to the power quality problems mitigation in energy storage system (ESS) in collaboration with Universiti Tenaga Nasional (UNITEN) and Universiti Kebangsaan Malaysia (UKM) under the Long Research Grant Scheme (LRGS), Ministry of Higher Education (MOHE). Furthermore, he has published more than 232 technical papers in international indexed journals and conferences. His research interests include electrical power systems, power system stability and reliability, power system deregulation, electricity market, enhanced energy efficiency technology, hybrid renewable energy, energy storage systems, active power filters, power quality, and artificial intelligence (AI).

SHEIKH TANZIM MERAJ received the B.Sc. degree in electrical and electronic engineering from the Ahsanullah University of Science and Technology, Dhaka, Bangladesh, in 2015, and the M.Eng. degree from the Department of Electrical and Computer Engineering, Curtin University, Miri, Malaysia, in 2018. He is currently a Graduate Assistant (GA) with the Department of Electrical and Electronic Engineering, University Technology PETRONAS (UTP), Perak, Malaysia, where he is also an Assistant Lecturer. He is actively involved in research-based work with specific research focuses on power electronics, power quality, renewable energy integration, energy management schemes, and hydrogen energy and applications. He is also an active reviewer of multiple IEEE TRANSACTIONS.

MASOUD AHMADIPOUR received the B.S. and M.S. degrees from Iran, in 2007 and 2011, respectively, and the Ph.D. degree from Universiti Putra Malaysia (UPM), Serdang, Selangor, Malaysia, in 2019, all in electrical engineering with a focus on power systems. He is currently an Associate Researcher with the Faculty of Electrical Engineering, University Teknologi MARA (UiTM), Shah Alam, Selangor, Malaysia. He is also attached to UiTM-Solar Energy Research (USER) Center. His research interests include renewable energy, power system analysis, power system protection, signal processing, computational intelligence, and smart grid.

M. S. HOSSAIN LIPU (Senior Member, IEEE) received the B.Sc. degree in electrical and electronic engineering from the Islamic University of Technology, Bangladesh, in 2008, the M.Sc. degree in energy from the Asian Institute of Technology, Thailand, in 2013, and the Ph.D. degree in electrical, electronic and systems engineering from the National University of Malaysia, in 2019. He is currently an Associate Professor with the Department of Electrical and Electronic Engineering, Green University of Bangladesh (GUB). Prior to joining GUB, he worked as a Senior Lecturer with the Department of Electrical, Electronic, and Systems Engineering, National University of Malaysia, and an Assistant Professor with the Department of Electrical and Electronic Engineering, University of Asia Pacific, Bangladesh. He has teaching experience at university for almost ten years in local and foreign universities. He secured a place in the list of the world's best 2 % scientists published by Stanford University and Elsevier, in 2022. He published numerous top-notch journals in IEEE TRANSACTIONS, Elsevier, and Nature Science. His research interests include battery storage and management systems, electrical vehicles, power electronics, intelligent controllers, artificial intelligence, and optimization in renewable systems. He won the best paper award in reputed IEEE conferences and was also awarded the gold medal in several exhibitions. He worked as the Track Chair and a Convener at the 4th International Conference on Sustainable Technologies for Industry 4.0 (STI 2022), organized by GUB. In addition, he worked as an invited speaker, the session chair at conferences, and a reviewer in top-ranked journals. He served as the guest editor for several renowned journals.
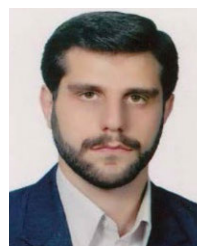
MOHSEN GITIZADEH was born in Iran, in February 1976. He received the B.S. degree in electrical engineering from Shiraz University, Shiraz, Iran, in 1999, and the M.S. and Ph.D. degrees from the Iran University of Science and Technology, in 2001 and 2009, respectively. He is currently a Professor with the Department of Electrical and Electronics Engineering, Shiraz University of Technology, Shiraz. His current research interests include power system operation and control, voltage stability, optimization, demand side management, and FACTS devices.

• • •